AGU Advances

COMMENTARY

10.1029/2020AV000376

Key Points:

- Meteorite paleomagnetism constrains the lifetime of the solar nebula and therefore the time by which Jupiter formed
- Jupiter's inferred growth rate supports the core accretion model for giant planet formation
- This proposal can be further tested with new measurements and theory constraining the origin of isotopic and magnetic records observed in meteorites

Supporting Information:

Supporting Information may be found in the online version of this article.

Correspondence to:

B. P. Weiss,
bpweiss@mit.edu

Citation:

Weiss, B. P., & Bottke, W. F. (2021). What can meteorites tell us about the formation of Jupiter? *AGU Advances*, *2*, e2020AV000376. https://doi.org/10.1029/2020AV000376

Received 18 DEC 2020
Accepted 22 APR 2021

Author Contributions:

Investigation: William F. Bottke
Validation: William F. Bottke
Writing – review & editing: William F. Bottke

What Can Meteorites Tell Us About the Formation of Jupiter?

Benjamin P. Weiss[1] **and William F. Bottke**[2]

[1]Department of Earth, Atmospheric, and Planetary Sciences, Massachusetts Institute of Technology, Cambridge, MA, USA, [2]Department of Space Studies, Southwest Research Institute, Boulder, CO, USA

Abstract Gas giants like Jupiter are a fundamental component of planetary systems, but how they formed has been uncertain. Here we discuss how paleomagnetic records in meteorites of the solar nebula may tell us about Jupiter's final growth stage. We suggest that under certain testable assumptions, the meteorite data indicate that proto-Jupiter grew from a mass of ~50 Earth masses ($M_\oplus$) at >3.46 million years (Ma) after solar system formation to its final mass of 318 $M_\oplus$ over just <0.5 Ma. This rapid acceleration is consistent with a key prediction of the core accretion model for giant planet formation.

Plain Language Summary Giant planets like Jupiter are composed largely of hydrogen and helium with small amounts of rocky and icy material. They formed from the gaseous reservoirs present during the formation stage of solar systems known as protoplanetary disks. Considerable theoretical progress has been made on understanding Jupiter's formation, yet there have been few observational constraints on its growth rate. In this Commentary, we synthesize meteorite compositional and magnetism data to glean insights into Jupiter's growth, arguing that Jupiter formed slowly over several million years before growing at least 30 times faster to reach its final mass. This long timescale and late, rapid acceleration match models showing that Jupiter formed first with the assembly of a rock-ice core followed by rapid accretion of gas. We can further test this idea with future astronomical observations of young star systems, magnetic measurements of meteorites, and theoretical studies that track the evolution of meteorite parent bodies.

1. Introduction

Understanding how giant planets like Jupiter and Saturn form is a longstanding fundamental problem in planetary science. Until recently, nearly all of our understanding of this question has been drawn from theoretical considerations, observations of the compositions and structures of giant planets, and astronomical observations of protoplanetary disks. In this Commentary, we consider what can be inferred about Jupiter's formation from a new and different kind of data set: the magnetism of meteorites. Although these rock samples of planetesimals might at first glance seem to have little relationship with the giant planets, they are a primary source of information about the age and nature of the solar nebula out of which the planets formed.

1.1. Giant Planet Formation Models

Gas giant planets are volatile-rich bodies with masses between ~0.1 and <~10–13 Jupiter-masses (1 Jupiter-mass = 318 Earth-masses [$M_\oplus$]) (Santerne, 2018; Schlaufman, 2018). Jupiter- and Saturn-like gas giants are thought to either possess ~0–25 $M_\oplus$ cores that are metal-rich (i.e., heavy element-rich) or at least deep interiors with a diffusely distributed enrichment of metals (Helled & Guillot, 2013; Wahl et al., 2017). Overlying these are hydrogen and helium envelopes with masses of tens to hundreds of $M_\oplus$.

There are two main formation models for giant planets: the gravitational (or disk) instability model (Kuiper, 1951) and core accretion model (Safronov, 1969) (Figure 1). In the gravitational instability model, a giant planet forms when the self-gravity of the gaseous nebula causes it to rapidly collapse (over <1,000 years) into a gravitationally bound clump, which then slowly cools and contracts. Gravitational instabilities capable of making giant planets are most likely to occur within spiral density anomalies (Helled et al., 2014). As

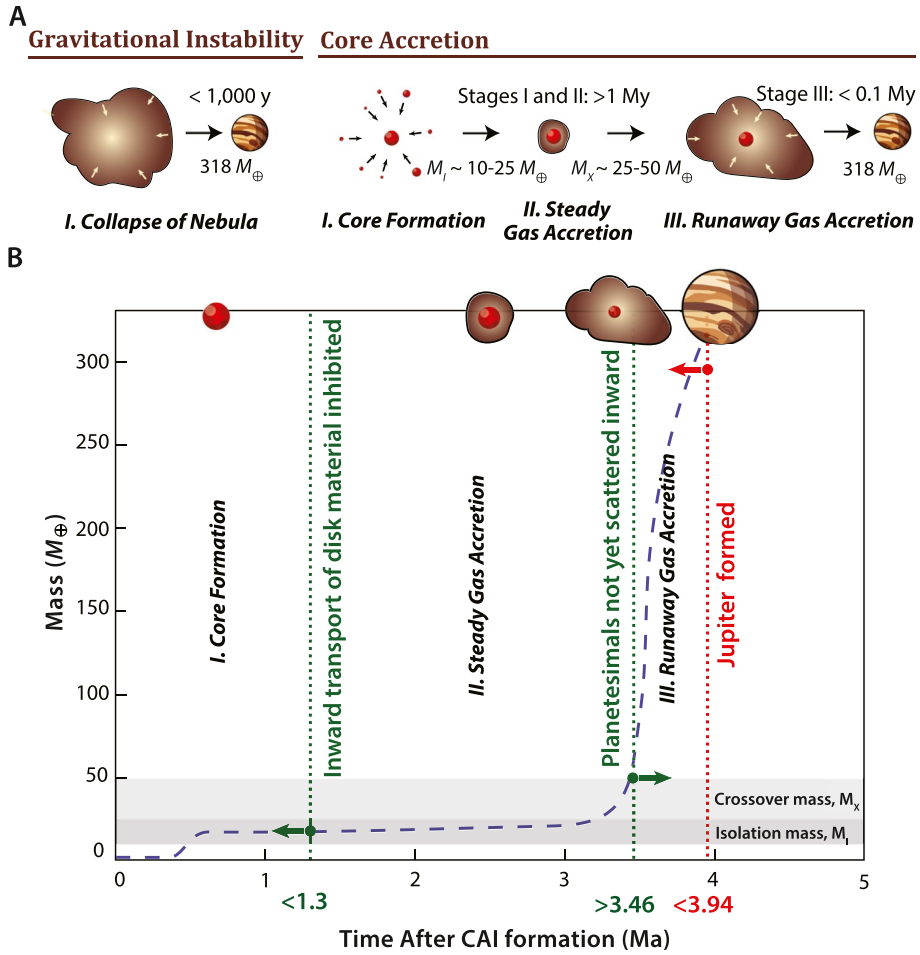

Figure 1. Formation of giant planets. (a) Theory. In the gravitational instability model (left), the nebula collapses to form a self-gravitating clump with the future planet's final mass (318 $M_\oplus$ for Jupiter) in <1,000 years. This clump then contracts to planet densities over 0.01–1 Ma (final phase not shown). The core accretion model has three stages (right). In stage I, a heavy element-rich core accretes until reaching the isolation mass, M_I. In stage II, the core slowly accretes a hydrostatically supported gaseous envelope until the body reaches the crossover mass, M_X. In stage III, the body experiences runaway gas accretion to its final mass in <0.1 Ma. (b) Schematic comparison of core accretion model for Jupiter (dashed curve) with proposed meteorite constraints. (a). The two shaded regions show the range of theoretical estimates for M_I and M_X. Regardless of their precise values, the accretion rate during phase III is expected to be at least 2 orders of magnitude faster than during the earlier phases. Combining isotopic constraints on the times of formation and duration of isolated nebular reservoirs (green) with paleomagnetic constraints on the lifetime of the nebula (red) suggests that proto-Jupiter grew from ~50 $M_\oplus$ sometime following 3.46 Ma after calcium aluminum-rich inclusion (CAI)-formation to its final mass of 318 $M_\oplus$ over a period of just <0.5 Ma, indicating a growth rate >30 times (and permissibly many orders of magnitude) higher than prior to this time.

discussed below, theoretical considerations indicate that relatively few giant planets should have formed by gravitational instabilities.

By comparison, core accretion is considered the most likely means to make giant planets in our planetary system and in the majority of exoplanet systems. While the gravitational instability model only has a single short phase of accretion, core accretion is typically thought to occur over three overlapping phases with vastly different durations (Alibert et al., 2018; Helled et al., 2014; Johansen & Lambrechts, 2017; Levison et al., 2015; Lissauer et al., 2009). In the first phase, pebbles (i.e., centimeter- to meter-sized rock-ice bodies) and planetesimals (i.e., ~1–1,000 km-sized rock-ice bodies) accrete relatively rapidly to form a dominantly metal-rich solid core. The mass of this core, known as the isolation mass M_I, is sufficiently large to produce a local pressure maximum in the nebula that deters further accretion of material coupled to the nebula (e.g., pebbles). Theory estimates that at a distance of 5–15 AU from the Sun, $M_I \approx 10 - 25 M_\oplus$ (Bitsch

et al., 2015; Johansen & Lambrechts, 2017; Lambrechts et al., 2014). Proto-Jupiter is theoretically expected to have reached this mass in own solar system at ∼0.5–1 Ma after the formation of calcium aluminum-rich inclusions (CAIs), the oldest known solar system solids.

In the second phase, gas slowly accretes along with additional solids until the body reaches the crossover mass, at which point the atmosphere's mass is comparable to that of the core: $M_X \approx 2M_I \approx 20 - 50\,M_\oplus$. In the third and last phase, runaway gas accretion at very rapid accretion rates ($\sim 10^2$–10^4 $M_\oplus$ Ma^{-1}) forms the final planet over a timescale that may only last the order of ∼0.1 Ma (Lissauer et al., 2009; Machida et al., 2010; Uribe et al., 2013; Venturini & Helled, 2020). A growing giant planet might skip the second core accretion phase if it experiences extensive orbital migration (Alibert et al., 2005; Helled et al., 2014) and/or the opacity of the accreting material is low (Hori & Ikoma, 2010). All told, core accretion is expected to last several Ma, depending on the lifetime and evolution of the solar nebula, with most of the planetary mass usually accreted during the runaway gas accretion stage.

1.2. Core Accretion Likely Made Most Known Giant Planets

At least for giant planets formed in situ within a few tens of AU of Sun-like stars, theoretical considerations strongly favor the core accretion model as the dominant mode of formation (e.g., Humphries et al. [2019]). A central difficulty with the gravitational instability model is that the inner regions of most disks around Sun-like stars lack sufficient disk surface densities to create giant planets due to the fact that gravity cannot overcome the opposing forces associated with disk shear and gas pressure (Williams & Cieza, 2011). For most disks older than ∼0.1 Ma, the critical surface density at which the gravitational instability can occur is unlikely to be achieved anywhere; the remainder of disks may achieve this critical surface density beyond a few tens of AU from the protostar where the gas may be sufficiently cool, assuming the disks extend this far (Durisen, 2011).

With respect to exoplanet observations, the relatively low abundance (Bowler, 2016) and steeply declining abundance with mass (Wagner et al., 2019) of distant giant planets both favor core accretion as the most common giant plant formation mechanism. In our solar system, the likely (although not certain) presence of $>10M_\oplus$ metal-rich cores in our four giant planets (D'Angelo & Lissauer, 2018), or at least diffuse heavy-element rich central regions (Wahl et al., 2017), is broadly consistent with the core accretion model. The core accretion model, which naturally produces relatively metal-rich planets, explains the frequency of occurrence of giant exoplanets (Fischer & Valenti, 2005) as well as their masses (Thorngren et al., 2016): both correlate with stellar metallicity, at least for planets with masses below a few Jupiter-masses (Helled et al., 2014; Humphries et al., 2019). The observation that most exoplanets with radii exceeding 1.6-Earth-radii (corresponding to 6 $M_\oplus$ for an Earth-like composition) have volatile-rich envelopes (Rogers, 2015) is also consistent with the predictions of the core accretion model (Lissauer et al., 2009).

1.3. Growth Timescales in Core Accretion Models

Core accretion likely requires ≥1 Ma for growth from planetesimals to masses exceeding the crossover mass (Helled et al., 2014; Johansen & Lambrechts, 2017; Lissauer et al., 2009). The combined duration of the first two phases of core accretion is thought to be at least an order of magnitude longer than the <∼0.1 Ma duration of the runaway gas accretion phase (Lissauer et al., 2009) (Figure 1). As such, whether and how core accretion formed Jupiter could be addressed with measurements of the tempo and duration of Jupiter's accretion.

However, at this time, there have been no previous studies that constrain the growth rate of Jupiter over the final stage of its formation when core accretion predicts runaway gas growth should have occurred. Here we discuss how, with certain testable assumptions, meteorite isotopic constraints on two intermediate phases of Jupiter's growth, combined with a meteorite paleomagnetic constraint on the birthdate of Jupiter, provide observational evidence for a runaway gas accretion stage on Jupiter, thereby fulfilling a key prediction of the core accretion model.

2. Meteorite Isotopic Constraints on the Early Growth of Jupiter

2.1. Growth to ~50 Earth Masses

Theoretical models indicate that after proto-Jupiter reached a critical mass, it should have opened up a gap in the nebular disk that may have chemically isolated the outer and inner solar system (Johansen & Lambrechts, 2017). Therefore, as recently proposed by Kruijer et al. (2017), by finding both the timing of the opening of this gap and its longevity, the mass of proto-Jupiter could be constrained at two different times during its growth.

The existence of such a gap in the disk has been inferred from the discovery that known meteorites are derived from two reservoirs with distinct O, Cr, Ti, Mo, Ni, and W isotopic compositions and whole (Mg-normalized) refractory lithophile element abundances (e.g., Kruijer et al., 2017; Nanne et al., 2019; Warren, 2011; Weisberg et al., 2006). These reservoirs are named for the chondrite classes found in each: one containing noncarbonaceous chondrites and the other containing carbonaceous chondrites. Although the precise formation locations of meteorites is a key uncertainty, the two reservoirs are generally thought to have been located at ~2–3 and perhaps >3–7 AU from the Sun for most meteorites (Desch et al., 2018; Sutton et al., 2017), with the possibility that some carbonaceous groups (e.g., CI, CR and CB chondrites and ungrouped Tagish Lake-like meteorites) formed at even greater distances (Bryson, Weiss, Biersteker, et al., 2020; Gounelle et al., 2006). Kruijer et al. (2017) proposed that the two reservoirs formed inward and outward of the formation location of proto-Jupiter, respectively, given that Jupiter is the largest giant planet and likely formed the largest core. This may not be required, though; the gap could have been created elsewhere, such as at the location of another forming giant planet or, more generally, anywhere there was a sufficiently large localized increase of pressure with distance (e.g., Brasser & Mojzsis [2020]). It is even possible the isotopic dichotomy can be explained without the need for a gap at all (Lichtenberg et al., 2021).

Iron meteorites, which are found in both the noncarbonaceous and carbonaceous reservoirs, are some of the oldest known meteorite samples and most are thought to represent the cores of differentiated planetesimals. Using isotopic measurements of iron meteorites combined with planetesimal thermal evolution models, Kruijer et al. (2017) calculated that noncarbonaceous and carbonaceous iron meteorite parent bodies had accreted by $0.9^{+0.4}_{-0.2}$ Ma after CAI-formation (95% confidence interval). The upper bound on this age suggests that the two reservoirs were isolated by <1.3 Ma after CAI-formation (Table S1). By this logic, proto-Jupiter reached its isolation mass of 10–25 $M_{\oplus}$ at this time (left green line in Figure 1b; Table S1).

The parent bodies of the ordinary chondrites, which are part of the noncarbonaceous reservoir, are estimated to have formed at ~2 Ma after CAI-formation (Kruijer et al. 2017). The youngest known carbonaceous chondrite parent body, that of the CR chondrites, is estimated to have accreted at 3.68 ± 0.22 Ma after CAI-formation (Kruijer et al., 2017) (Weiss et al. [2021], Table S1). Therefore, taking the 95% confidence lower bound on the latter age, this suggests that the two nebular reservoirs remained isolated and spatially separated until >3.46 Ma after CAI-formation (right green line in Figure 1b; Table S1).

Kruijer et al. (2017) hypothesized that proto-Jupiter must have reached ~50 $M_{\oplus}$ after this time because otherwise it would have likely scattered nearby planetesimals, mixing the reservoirs in a manner that might have influenced or interfered with the formation of CR chondrites (Figure 1b). Such scattering could occur via the migration of proto-Jupiter (Walsh et al., 2011) and/or direct gravitational interactions from a static Jupiter (Raymond & Izidoro, 2017). On the other hand, proto-Jupiter may have begun scattering planetesimals at a lower mass (e.g., during an earlier epoch of migration), in which case Jupiter's mass could have been as low as ~10 $M_{\oplus}$ at this time (i.e., the mass limit inferred from the accretion of carbonaceous iron meteorite parent bodies).

2.2. Lack of Constraints on Growth From ~50 to 318 Earth Masses

All told, Kruijer et al. (2017) argued that the isotopic data constrain the formation of Jupiter at two intermediate stages of its growth: the body reached ~10–25 $M_{\oplus}$ by 1.3 Ma after CAI-formation and ~50 $M_{\oplus}$ after 3.46 Ma after CAI-formation. However, as discussed above, while the isotopic measurement themselves are robust, their causal connection with the opening of a gap in the nebula around proto-Jupiter and their

proposed implications for proto-Jupiter's growth are far from conclusive (see also Kruijer et al. [2019] and Klein et al. [2020]). We revisit these and other uncertainties at the end of this Commentary. For now, we assume the validity of their constraints on Jupiter's accretion and explore their implications for Jupiter's formation in the context of meteorite paleomagnetic measurements.

Recent models assuming pebble accretion during the first stage followed by accretion dominated by planetesimals during the second stage can successfully match the growth rates during these two stages implied by the isotopic data (Alibert et al., 2018). Specifically, these models reproduce the >2 Ma-long growth period to ~50 $M_{\oplus}$ inferred from the isotopic data (Kruijer et al., 2017). Even so, the isotopic data only constrain the growth of Jupiter to just 15% of its final mass, leaving the timing of most of the growth of Jupiter unconstrained.

Given that the core accretion model predicts that Jupiter's growth accelerated significantly after it reached ~50 $M_{\oplus}$ due to the onset of runaway gas accretion, it is critical to determine the subsequent and final period of Jupiter's growth to ~318 $M_{\oplus}$ (Ginzburg & Chiang, 2019; Hubickyj et al., 2005; Lissauer et al., 2009; Venturini & Helled, 2020). At present, models tend to force the accretion rate to zero at ~3–5 Ma time after CAI-formation. This timing is chosen to prevent the final mass from exceeding ~318 $M_{\oplus}$ and relies on the common assumption that the nebula dispersed at this time. However, such a solar nebula lifetime is an inference based on astronomical observations indicating that half of all protoplanetary disks disperse somewhere between ~2 and 6 Ma after formation, with this large range due to uncertainties in age models of young stellar objects (Bell et al., 2013; Mamajek, 2009). Not only is this mean disk lifetime uncertain by several Ma, but where the lifetime of our solar nebula falls in this distribution is also not well-known.

Other than inferences inferred from the observed lifetimes of protoplanetary disks, there have been very few constraints on the lifetime of the solar nebula. The presence of agglomeratic olivine chondrules in CR chondrites has been interpreted as evidence that the nebular dust disk persisted until at least the formation time of CR chondrules (Schrader et al., 2018) (i.e., at >3.46 Ma) (Table S1). It has also been proposed that the formation of chondrules in CH and CB chondrites requires the presence of nebular gas under the hypothesis that they are impact melt sprays from planetesimal collisions (Krot et al., 2005). Such gas could not only potentially enable planetesimals to reach the high relative velocities that can produce such impacts (Johnson et al., 2016) but would also enable the reaccretion of such chondrules onto the CH/CB parent body (Garvie et al., 2017; Morris et al., 2015). This may indicate that the solar nebula persisted until the ~4–6 Ma formation age of CB chondrules (Bollard et al., 2017; Wölfer et al., 2020) (Table S1 and Table S1 of Weiss et al. [2021]).

Determining the lifetime of our solar nebula and, by implication, the end date of Jupiter's growth, is important for multiple reasons. Most importantly, this provides an experimental test of the core accretion model. Given that core accretion models typically rely on the disappearance of the nebular to truncate Jupiter's growth, our understanding of the runaway gas accretion stage might require modification if it were found that the solar nebula had lasted ~>10 Ma after CAI formation. Beyond setting limits on the mass of Jupiter, a long-lived nebula could produce eccentricity and inclination damping of planetesimal and planetary orbits until ~>10 Ma after CAI-formation, delaying the onset of giant planet dynamical instabilities and post-nebular migration (e.g., Nesvorný et al. [2021]). Such an outcome might could affect critical terrestrial planet formation timescales, the timing of the giant impact that produced the Moon, and the dispersal of small bodies produced by giant planet migration.

Accordingly, we now discuss how recent meteorite paleomagnetic data have directly constrained the lifetime our nebula. This will potentially enable us to estimate Jupiter's accretion rate in its final growth stage without requiring inferences from astronomical observations of other disks.

3. Meteorite Paleomagnetism

3.1. Evidence for a Nebular Magnetic Field

Theoretical studies predict that the solar nebula likely generated a large-scale magnetic field that played a central role in stellar accretion (Turner et al., 2014). For decades, a key goal of meteorite paleomagnetic studies has been to search for evidence of this field, but ambiguities associated with the age of measured

magnetization records and the ability to accurately infer ancient field intensities (paleointensities) meant that until recently, no nebular field records were unambiguously identified (Cisowski, 1987; Weiss et al., 2010).

However, with the recent advent of high sensitivity magnetometers, new microsampling tools, high resolution magnetic imaging, and the advantage provided by decades of mineralogical and geochemical studies of meteorites, nebular field records have finally been identified. In particular, it has been found that LL (Fu et al., 2014; Mai et al., 2018) and CM (Cournède et al., 2015) chondrites recorded a midplane field of 54 ± 21 μT and $\gtrsim$6 μT at 2.03 ± 0.81 Ma and 2.90 ± 0.39 Ma after CAI formation, respectively (Table S1 of Weiss et al. [2021]).

Just as for meteorite isotopic constraints, a difficulty in interpreting meteorite magnetic constraints is that it is not known where exactly in the disk they apply. Here we make the assumption that the constraints apply to the parent isotopic reservoirs of the bulk meteorites, which are the noncarbonaceous and carbonaceous reservoirs for LL and CM chondrites, respectively. In this case, taking the 95% confidence lower limits, these data indicate the nebula persisted until >1.22 and >2.51 Ma after CAI formation in these two reservoirs (Table S1 and Figure 7 of Weiss et al. [2021]).

Note that although it was alternatively proposed that CM chondrites were magnetized by the ancient solar wind after the nebula had dispersed (O'Brien et al., 2020), this is unlikely because even if the nebula had cleared by the time CMs were magnetized, the time-averaged solar wind field at 2 AU was likely >2 orders of magnitude too weak to explain the minimum CM paleointensities (Oran et al., 2018). Furthermore, at the inferred 2.90 ± 0.39 Ma magnetization time of CM chondrites, the nebula was likely still present and would have shielded them against the solar wind (Weiss et al., 2021).

Knowledge of magnetic field paleointensities does not directly constrain the nebular gas density. However, because magnetic fields can exert torques on ionized gas, the midplane magnetic field strength can be used to infer the accretion rate under the assumption that magnetic fields mediated accretion (Weiss et al., 2021). The accretion rate, in turn, is a broadly a proxy for the gas density. As such, the LL and minimum CM chondrule paleointensities indicate accretion rates of $\sim 10^{-9}$ to $10^{-8}\ M_{\odot}\mathrm{y}^{-1}$ and $> 10^{-9}\ M_{\odot}\mathrm{y}^{-1}$, respectively. These are consistent with astronomical observations of typical actively accreting protoplanetary disks throughout most of their lifetimes (Hartmann et al., 1998) and support the persistence of the nebula until at least these times. Therefore, the 95% confidence lower limits on the ages of LL and CM chondrules indicate lower limits of 1.22 and 2.51 Ma on the lifetime of the nebula in the noncarbonaceous and carbonaceous reservoirs, respectively.

3.2. Paleomagnetic Constraints on the Lifetime of the Nebula

Because the sustenance of magnetic fields requires a conducting medium, the solar nebula dispersal time can be estimated by determining when nebular fields disappeared as inferred from the presence and absence of paleomagnetism in meteorites of different ages (Wang et al., 2017). In particular, paleomagnetic studies of angrites, which formed in the noncarbonaceous reservoir, indicate the nebular field intensity had dropped to <0.6 μT by 3.71 ± 0.23 Ma after CAI-formation (Table S1 and Figure 7 of Weiss et al. [2021]). Likewise, paleomagnetic studies of the CV chondrite Kaba, which formed in the carbonaceous reservoir, indicate the field was <0.3 μT by 4.08 ± 0.81 Ma after CAI-formation (Table S1 and Figure 7 of Weiss et al. [2021]).

If we again assume that magnetic fields mediated stellar accretion (Weiss et al., 2021), these factors of >∼90 and >∼20 decrease in paleointensities relative to those just 1–3 Ma earlier would indicate that the accretion rate had dropped by this time by factors of >8,000 and >400 in the noncarbonaceous and carbonaceous reservoirs, respectively. Such low accretion rates are, respectively, at least 3 and 2 orders of magnitude below those inferred for typical disks and also below those observed for the slowest-known accreting disks (Ercolano & Pascucci, 2017; Espaillat et al., 2014; Owen, 2016).

The meteorite paleomagnetic data therefore indicate that the nebula had already dissipated by the time these near-zero magnetic field conditions were recorded. Combining the age uncertainties on the angrites

and the CV chondrite, we therefore place 95% confidence upper limits on the lifetime of the nebula in the noncarbonaceous and carbonaceous reservoirs of 3.94 and 4.89 Ma after CAI-formation, respectively. Overall, the results suggest that the nebula had at least locally dispersed sometime between >1.22 and <3.94 Ma after CAI-formation in the noncarbonaceous reservoir and between >2.51 and <4.89 Ma in the carbonaceous reservoir (95% confidence limits) (Figure 1b and Table S1).

4. Meaning for Jupiter's Formation Mechanism

The minimum 1.22 and 1.3 Ma lifetimes of the nebula inferred from meteorite paleomagnetism and meteorite isotopic studies, respectively, are consistent with predictions of the core accretion model. The isotopic measurements more specifically suggest that Jupiter grew from 0 to 10–25 $M_{\oplus}$, the range of masses theoretically predicted for the end of core accretion's first phase, at a mean accretion rate of >7.7–19.2 $M_{\oplus}$ Ma^{-1} (to first green line in Figure 1b; Table S1) and then from 10–25 to 50 $M_{\oplus,}$ the upper end of the range of masses for the end of the second phase, at a mean rate of <11.8–18.8 $M_{\oplus}$ Ma^{-1} (between two green lines in Figure 1b; Table S1).

The combined isotopic and paleomagnetic measurements (between right green and red lines in Figure 1b) indicate that Jupiter grew from 50 $M_{\oplus}$ to its final mass of ∼318 $M_{\oplus}$ at a mean growth rate of >518 $M_{\oplus}$ Ma^{-1} (Table S1). Both the magnitude of the latter growth rate as well as the rapid increase in growth rate relative to the previous growth phase (by a minimum factor of ∼30 and permissibly by many orders of magnitude) are consistent with typical models of core accretion, which predict runaway gas accretion rates ∼2–4 orders of magnitude faster than during the slow gas accretion phase (Machida et al., 2010; Venturini & Helled, 2020). The timing of the initiation of runaway gas accretion is insensitive to the choice of chronometers for dating CR chondrules and angrites, to uncertainties associated with the age of CAIs (Table S1), and to the factor of ∼2 uncertainty associated with the estimates of the isolation and crossover masses. We caution, however, that these ages provide a poorer fit to model variants in which the slow gas accretion phase is suppressed by substantial migration (Helled et al., 2014).

5. Assumptions and Path Forward

While the match between core accretion model predictions and meteorite observations is excellent, this outcome does rely on several assumptions that should be evaluated by future studies. First, the assumption that the growth of a giant planet led to the formation of the two isotopic reservoirs needs to be validated. Our understanding of the nature and mechanisms for forming pressure bumps in disk is advancing rapidly due spatially resolved observations of disks with substructures by the Atacama Large Millimeter/submillimeter Array (Andrews, 2020).

Second, Kruijer et al. (2017)'s proposal that the isotopic data constrain growth to 50 $M_{\oplus}$ assumes that the noncarbonaceous reservoir would be contaminated by material from the carbonaceous reservoir due to proto-Jupiter's scattering of planetesimals. However, substantial contamination of the noncarbonaceous reservoir would likely require extensive collisional evolution of carbonaceous planetesimals in the same region where new planetesimals were forming within the nebula. No study has yet investigated whether such conditions are likely to take place. Furthermore, it is not guaranteed that noncarbonaceous bodies were still accreting when the putative contamination phase could have taken place. Finally, the growth of the other giant planets may have also regulated mixing of the two reservoirs (Raymond & Izidoro, 2017). These assumptions could be addressed with dynamical models of giant planet growth, planetesimal scattering and planetesimal collisional evolution.

Third, we again emphasize that the solar system locations where meteorites obtained their paleomagnetic records are poorly known. Here we assumed that meteorites that acquired their magnetic records in the noncarbonaceous or carbonaceous reservoirs actually provide a snapshot of nebular activities throughout that reservoir. This may be valid in the more confined regions of the inner solar system, but the outer solar system spans an enormous distance, ranging from Jupiter to the Kuiper belt. The nebula dissipation constraints from CV, CH, and CB chondrites might therefore apply to different portions of this vast region. On the other hand, it is also possible, for example, that CV chondrites were remagnetized after injection

into the asteroid belt. A possible way of resolving this issue is to use the predicted dependency of nebular field strength with distance (Weiss et al., 2021) to constrain the formation distance of a particular magnetic record. As an example, it was recently argued that the weak nebular field recorded by ungrouped Tagish Lake-like chondrites indicates they formed beyond ~10 AU, consistent with their volatile-rich compositions and extreme 15 N-isotopic compositions (Bryson, Weiss, Biersteker, et al., 2020; Bryson, Weiss, Lima, et al., 2020). On the other hand, this predicted field dependency on distance assumes constant accretion rates in space and time (Fu et al., 2020).

6. Conclusions and Implications

Under several testable assumptions, the meteorite constraints on Jupiter's growth over time match predictions from the core accretion model. There are two principle reasons for this. First, as noted by Kruijer et al. (2017), the isotopic data indicate that the overall growth timescale of Jupiter was protracted (>1 Ma). Second, as introduced here, the combined isotopic and paleomagnetic data indicate that the growth rate greatly accelerated soon after reaching a mass comparable to the expected crossover mass, as expected after the onset of runaway gas accretion.

The paleomagnetic data also constrain an important aspect of the runaway gas accretion phase in the core accretion model. It has long been suggested that Jupiter's growth in this phase was ultimately terminated because the body emptied its neighborhood of gas (Ginzburg & Chiang, 2019; Lissauer et al., 2009). Our analysis of the meteorite record supports this: we find the time of dissipation of the nebula is within error of both the time that Jupiter reached its final mass and the time it reached its crossover mass.

Formation of Jupiter by core accretion has several additional important implications. It means that Jupiter formed with, and likely still contains, a heavy element-rich deep interior of at least several tens of $M_{\oplus}$, a structure that has been challenging to ascertain with gravity field measurements (Wahl et al., 2017). It also provides increasing evidence that core accretion is a widespread process for forming giant planets. Giant planet formation may therefore be frustrated in exoplanet systems in which the gaseous protoplanetary disk dissipates rapidly (<1 Ma after formation) and/or around metal-poor stars. Nevertheless, giant planet formation by core accretion remains challenging at large (>100 AU) distances from the central star. The giant planets that have been directly imaged in these locations (Marois et al., 2010) may have formed either in situ by the gravitational instability (Durisen, 2011) or else may formed in the inner solar system or another star system and then migrated or were scattered to their present positions (Ford, 2014).

Conflict of Interest

The authors declare no conflicts of interest relevant to this study.

Data Availability Statement

All the data presented in this paper are drawn from previously published studies cited in the paper.

Acknowledgments
The authors thank J. Biersteker, C. Borlina, S. Desch, A. Johansen, N. Kita, O. Pravdivtseva, S. T. Stewart, F. Tissot, J. Wisdom, and anonymous reviewers of earlier versions of this manuscript for helpful comments and B. Carbone and M. Parsons for administrative support. B. P. Weiss thanks the NASA Emerging Worlds program (grant number NNX15AH72G) and Thomas F. Peterson, Jr. for support. The authors thank B. Ehlmann and F. Nimmo for editing this Commentary.

References

Alibert, Y., Mordasini, C., Benz, W., & Winisdoerffer, C. (2005). Models of giant planet formation with migration and disc evolution. *Astronomy and Astrophysics*, *434*, 343–353. https://doi.org/10.1051/0004-6361:20042032

Alibert, Y., Venturini, J., Helled, R., Ataiee, S., Burn, R., Senecal, L., et al. (2018). The formation of Jupiter by hybrid pebble-planetesimal accretion. *Nature Astronomy*, *2*, 873–877. https://doi.org/10.1038/s41550-018-0557-2

Andrews, S. M. (2020). Observations of protoplanetary disk structures. *Annual Review of Astronomy and Astrophysics*, *58*, 483–528. https://doi.org/10.1146/annurev-astro-031220-010302

Bell, C. P. M., Naylor, T., Mayne, N. J., Jeffries, R. D., & Littlefair, S. P. (2013). Pre-main-sequence isochrones - II. Revising star and planet formation time-scales. *Monthly Notices of the Royal Astronomical Society*, *434*, 806–831. https://doi.org/10.1093/mnras/stt1075

Bitsch, B., Johansen, A., Lambrechts, M., & Morbidelli, A. (2015). The structure of protoplanetary discs around evolving young stars. *Astronomy and Astrophysics*, *575*, A28. https://doi.org/10.1051/0004-6361/201424964

Bollard, J., Connelly, J. N., Whitehouse, M. J., Pringle, E. A., Bonal, L., Jørgensen, J. K., et al. (2017). Early formation of planetary building blocks inferred from Pb isotopic ages of chondrules. *Science Advances*, *3*, e1700407. https://doi.org/10.1126/sciadv.1700407

Bowler, B. P. (2016). Imaging extrasolar giant planets. *Publications of the Astronomical Society of the Pacific*, *128*, 102001. https://doi.org/10.1088/1538-3873/128/968/102001

Brasser, R., & Mojzsis, S. J. (2020). The partitioning of the inner and outer Solar System by a structured protoplanetary disk. *Nature Astronomy*, *4*, 492–499. https://doi.org/10.1038/s41550-019-0978-6

Bryson, J. F. J., Weiss, B. P., Biersteker, J. B., King, A. J., & Russell, S. S. (2020). Constraints on the distances and timescales of solid migration in the early solar system from meteorite magnetism. *The Astrophysical Journal*, *896*, 103. https://doi.org/10.3847/1538-4357/ab91ab

Bryson, J. F. J., Weiss, B. P., Lima, E. A., Gattacceca, J., & Cassata, W. S. (2020). Evidence for asteroid scattering and distal solar system solids from meteorite paleomagnetism. *The Astrophysical Journal*, *892*, 126. https://doi.org/10.3847/1538-4357/ab7cd4

Cisowski, S. M. (1987). Magnetism of meteorites. In Jacobs, J. A. (Ed.), *Geomagnetism, Volume 2*. (pp. 525–560). London: Academic Press.

Cournède, C., Gattacceca, J., Gounelle, M., Rochette, P., Weiss, B. P., & Zanda, B. (2015). An early solar system magnetic field recorded in CM chondrites. *Earth and Planetary Science Letters*, *410*, 62–74. https://doi.org/10.1016/j.epsl.2014.11.019

D'Angelo, G., & Lissauer, J. J. (2018). Formation of giant planets. In Deeg, H. J., & Belmonte, J. A. (Eds.), *Handbook of Exoplanets* (pp. 2319–2343). Springer.

Desch, S. J., Kalyaan, A., & Alexander, C. M. O. D. (2018). The effect of Jupiter's formation on the distribution of refractory elements and inclusions in meteorites. *The Astrophysical Journal Supplement Series*, *238*, 11. https://doi.org/10.3847/1538-4365/aad95f

Durisen, R. H. (2011). Disk hydrodynamics. In Garcia, P. J. V. (Ed.), *Physical Processes in Circumstellar Disks* (pp. 149–236). Chicago: University of Chicago Press.

Ercolano, B., & Pascucci, I. (2017). The dispersal of planet-forming discs: Theory confronts observations. *Royal Society of Open Science*, *4*, 170114. https://doi.org/10.1098/rsos.170114

Espaillat, C., Muzerolle, J., Najita, J., Andrews, S., Zhu, Z., Calvet, N., et al. (2014). An observational perspective of transitional disks. In Beuther, H, Klessen, R. S., Dullemond, C. P., & Henning, T. (Eds.), *Protostars and Planets VI* (pp. 497–520). Tucson: University of Arizona Press.

Fischer, D. A., & Valenti, J. (2005). The Planet-Metallicity Correlation. *The Astrophysical Journal*, *622*, 1102–1117. https://doi.org/10.1086/428383

Ford, E. B. (2014). Architectures of planetary systems and implications for their formation. *Proceedings of the National Academy of Sciences*, *111*, 12616–12621. https://doi.org/10.1073/pnas.1304219111

Fu, R. R., Kehayias, P., Weiss, B. P., Schrader, D. L., Bai, X.-N., & Simon, J. B. (2020). Weak magnetic fields in the outer solar nebular recorded in CR chondrites. *Journal of Geophysical Research*, *125*, e2019JE006260. https://doi.org/10.1029/2019je006260

Fu, R. R., Weiss, B. P., Lima, E. A., Harrison, R. J., Bai, X.-N., Desch, S. J., et al. (2014). Solar nebula magnetic fields recorded in the Semarkona meteorite. *Science*, *346*, 1089–1092. https://doi.org/10.1126/science.1258022

Garvie, L. A. J., Knauth, L. P., & Morris, M. A. (2017). Sedimentary laminations in the Isheyevo (CH/CBb) carbonaceous chondrite formed by gentle impact-plume sweep-up. *Icarus*, *292*, 36–47. https://doi.org/10.1016/j.icarus.2017.03.021

Ginzburg, S., & Chiang, E. (2019). The end of runaway: How gap opening limits the final masses of gas giants. *Monthly Notices of the Royal Astronomical Society*, *487*, 681–690. https://doi.org/10.1093/mnras/stz1322

Gounelle, M., Spurný, P., & Bland, P. A. (2006). The orbit and atmospheric trajectory of the Orgueil meteorite from historical records. *Meteoritics & Planetary Sciences*, *41*, 135–150. https://doi.org/10.1111/j.1945-5100.2006.tb00198.x

Hartmann, L., Calvet, N., Gullbring, E., & D'Alessio, P. (1998). Accretion and the evolution of T Tauri disks. *The Astrophysical Journal*, *495*, 385–400. https://doi.org/10.1086/305277

Helled, R., Bodenheimer, P., Podolak, M., Boley, A., Meru, F., Nayakshin, S., et al. (2014). Giant planet formation, evolution, and internal structure. In Beuther, H., Dullemond, C. P., Klessen, R. S., & Henning, T. K. (Eds.), *Protostars and Planets VI* (pp. 643–666). Tucson: University of Arizona Press.

Helled, R., & Guillot, T. (2013). Interior models of Saturn: Including the uncertainties in shape and rotation. *The Astrophysical Journal*, *767*, 113. https://doi.org/10.1088/0004-637x/767/2/113

Hori, Y., & Ikoma, M. (2010). Critical core masses for gas giant formation with grain-free envelopes. *The Astrophysical Journal*, *714*, 1343–1346. https://doi.org/10.1088/0004-637x/714/2/1343

Hubickyj, O., Bodenheimer, P., & Lissauer, J. (2005). Accretion of the gaseous envelope of Jupiter around a 5–10 Earth-mass core. *Icarus*, *179*, 415–431. https://doi.org/10.1016/j.icarus.2005.06.021

Humphries, J., Vazan, A., Bonavita, M., Helled, R., & Nayakshin, S. (2019). Constraining the initial planetary population in the gravitational instability model. *Monthly Notices of the Royal Astronomical Society*, *488*, 4873–4889. https://doi.org/10.1093/mnras/stz2006

Johansen, A., & Lambrechts, M. (2017). Forming planets via pebble accretion. *Annual Review of Earth and Planetary Sciences*, *45*, 359–387. https://doi.org/10.1146/annurev-earth-063016-020226

Johnson, B. C., Walsh, K. J., Minton, D. A., Krot, A. N., & Levison, H. F. (2016). Timing of the formation and migration of giant planets as constrained by CB chondrites. *Science Advances*, *2*, e1601658. https://doi.org/10.1126/sciadv.1601658

Kleine, T., Budde, G., Burkhardt, C., Kruijer, T. S., Worsham, E. A., Morbidelli, A., & Nimmo, F. (2020). The non-carbonaceous–carbonaceous meteorite dichotomy. *Space Science Reviews*, *216*, 55. https://doi.org/10.1007/s11214-020-00675-w

Krot, A. N., Amelin, Y., Cassen, P., & Meibom, A. (2005). Young chondrules in CB chondrites from a giant impact in the early Solar System. *Nature*, *436*, 989–992. https://doi.org/10.1038/nature03830

Kruijer, T. S., Burkhardt, C., Budde, G., & Kleine, T. (2017). Age of Jupiter inferred from the distinct genetics and formation times of meteorites. *Proceedings of the National Academy of Sciences of the United States of America*, *114*, 201704461. https://doi.org/10.1073/pnas.1704461114

Kruijer, T. S., Kleine, T., & Borg, L. E. (2019). The great isotopic dichotomy of the early solar system. *Nature Astronomy*, *4*, 32–40. https://doi.org/10.1038/s41550-019-0959-9

Kuiper, G. P. (1951). On the origin of the solar system. *Proceedings of the National Academy of Sciences*, *37*, 1–14. https://doi.org/10.1073/pnas.37.1.1

Lambrechts, M., Johansen, A., & Morbidelli, A. (2014). Separating gas-giant and ice-giant planets by halting pebble accretion. *Astronomy and Astrophysics*, *572*, A35. https://doi.org/10.1051/0004-6361/201423814

Levison, H. F., Kretke, K. A., & Duncan, M. J. (2015). Growing the gas-giant planets by the gradual accumulation of pebbles. *Nature*, *524*, 322–324. https://doi.org/10.1038/nature14675

Lichtenberg, T., Drążkowska, J., Schönbächler, M., Golabek, G. J., & Hands, T. O. (2021). Bifurcation of planetary building blocks during Solar System formation. *Science*, *371*, 365–370. https://doi.org/10.1126/science.abb3091

Lissauer, J. J., Hubickyj, O., D'Angelo, G., & Bodenheimer, P. (2009). Models of Jupiter's growth incorporating thermal and hydrodynamic constraints. *Icarus*, *199*, 338–350. https://doi.org/10.1016/j.icarus.2008.10.004

Machida, M. N., Kokubo, E., Inutsuka, S., & Matsumoto, T. (2010). Gas accretion onto a protoplanet and formation of a gas giant. *Monthly Notices of the Royal Astronomical Society*, *405*, 1227–1243.

Mai, C., Desch, S. J., Boley, A. C., & Weiss, B. P. (2018). Magnetic fields recorded by chondrules formed in nebular shocks. *The Astrophysical Journal*, *857*, 96. https://doi.org/10.3847/1538-4357/aab711

Mamajek, E. E. (2009). Initial conditions of planet formation: Lifetimes of primordial disks. In Usuda, T., Ishii, M., & Tamura, M. (Eds.), *Exoplanets and Disks: Their Formation and Diversity* (pp. 3–10). American Institute of Physics.

Marois, C., Zuckerman, B., Konopacky, Q. M., Macintosh, B., & Barman, T. (2010). Images of a fourth planet orbiting HR 8799. *Nature*, *468*, 1080–1083. https://doi.org/10.1038/nature09684

Morris, M. A., Garvie, L. A. J., & Knauth, L. P. (2015). New insight into the solar system's transition disk phase provided by the metal-rich carbonaceous chondrite Isheyevo. *The Astrophysical Journal Letters*, *801*. https://doi.org/10.1088/2041-8205/1801/1082/L102210.1088/2041-8205/801/2/l22

Nanne, J. A. M., Nimmo, F., Cuzzi, J. N., & Kleine, T. (2019). Origin of the non-carbonaceous-carbonaceous meteorite dichotomy. *Earth and Planetary Science Letters*, *511*, 44–54. https://doi.org/10.1016/j.epsl.2019.01.027

Nesvorný, D., Roig, F. V., & Deienno, R. (2021). The role of early giant-planet instability in terrestrial planet formation. *The Astronomical Journal*, *161*, 50. https://doi.org/10.3847/1538-3881/abc8ef

O'Brien, T., Tarduno, J. A., Anand, A., Smirnov, A. V., Blackman, E. G., Carroll-Nellenback, J., & Krot, A. N. (2020). Arrival and magnetization of carbonaceous chondrites in the asteroid belt before 4562 million years ago. *Communications Earth & Environment*, *1*, 54.

Oran, R., Weiss, B. P., & Cohen, O. (2018). Were chondrites magnetized by the early solar wind? *Earth and Planetary Science Letters*, *492*, 222–231. https://doi.org/10.1016/j.epsl.2018.02.013

Owen, J. E. (2016). The origin and evolution of transition discs: Successes, problems, and open questions. *PASA: Publications of the Astronomical Society of Australia*, *33*, e005. https://doi.org/10.1017/pasa.2016.2

Raymond, S. N., & Izidoro, A. (2017). Origin of water in the inner Solar System: Planetesimals scattered inward during Jupiter and Saturn's rapid gas accretion. *Icarus*, *297*, 134–148. https://doi.org/10.1016/j.icarus.2017.06.030

Rogers, L. A. (2015). Most 1.6 Earth-radius planets are not rocky. *The Astrophysical Journal*, *801*, 41. https://doi.org/10.1088/0004-637x/801/1/41

Safronov, V. S. (1969). *Evolution of the Protoplanetary Cloud and Formation of the Earth and planets*. Moscow: Nauka.

Santerne, A. (2018). Populations of extrasolar giant planets from transit and radial velocity surveys. In Deeg, H. J., & Belmonte, J. A. (Eds.), *Handbook of Exoplanets* (pp. 1–23). Springer. https://doi.org/10.1007/978-3-319-30648-3_154-1

Schlaufman, K. C. (2018). Evidence of an upper bound on the masses of planets and its implications for giant planet formation. *The Astrophysical Journal*, *853*, 37. https://doi.org/10.3847/1538-4357/aa961c

Schrader, D. L., Nagashima, K., Waitukaitis, S. R., Davidson, J., McCoy, T. J., Connolly, H. C., & Lauretta, D. S. (2018). The retention of dust in protoplanetary disks: Evidence from agglomeratic olivine chondrules from the outer Solar System. *Geochimica et Cosmochimica Acta*, *223*, 405–421. https://doi.org/10.1016/j.gca.2017.12.014

Sutton, S., Alexander, C. M. O. D., Bryant, A., Lanzirotti, A., Newville, M., & Cloutis, E. A. (2017). The bulk valence state of Fe and the origin of water in chondrites. *Geochimica et Cosmochimica Acta*, *211*, 115–132. https://doi.org/10.1016/j.gca.2017.05.021

Thorngren, D. P., Fortney, J. J., Murray-Clay, R. A., & Lopez, E. D. (2016). The mass-metallicity relation for giant planets. *The Astrophysical Journal*, *831*, 64. https://doi.org/10.3847/0004-637x/831/1/64

Turner, N. J., Fromang, S., Gammie, C., Klahr, H., Lesur, G., Wardle, M., & Bai, X.-N. (2014). Transport and accretion in planet-forming disks. In H. Beuther, R. S. Klessen, C. P. Dullemond & T. Henning (Eds.), *Protostars and Planets VI* (pp. 411–432). Tucson: University of Arizona Press.

Uribe, A. L., Klahr, H., & Henning, T. (2013). Accretion of gas onto gap-opening planets and circumplanetary flow structure in magnetized turbulent disks. *The Astrophysical Journal*, *769*, 97. https://doi.org/10.1088/0004-637x/769/2/97

Venturini, J., & Helled, R. (2020). Jupiter's heavy-element enrichment expected from formation models. *Astronomy and Astrophysics*, *634*, A31. https://doi.org/10.1051/0004-6361/201936591

Wagner, K., Apai, D., & Kratter, K. M. (2019). On the mass function, multiplicity, and origins of wide-orbit giant planets. *The Astrophysical Journal*, *877*, 46. https://doi.org/10.3847/1538-4357/ab1904

Wahl, S. M., Hubbard, W. B., Militzer, B., Guillot, T., Miguel, Y., Movshovitz, N., et al. (2017). Comparing Jupiter interior structure models to Juno gravity measurements and the role of a dilute core. *Geophysical Research Letters*, *44*, 4649–4659. https://doi.org/10.1002/2017gl073160

Walsh, K. J., Morbidelli, A., Raymond, S. N., O'Brien, D. P., & Mandell, A. M. (2011). A low mass for Mars from Jupiter's early gas-driven migration. *Nature*, *475*, 206–209. https://doi.org/10.1038/nature10201

Wang, H., Weiss, B. P., Bai, X.-N., Downey, B. G., Wang, J., Wang, J., et al. (2017). Lifetime of the solar nebula constrained by meteorite paleomagnetism. *Science*, *355*, 623–627. https://doi.org/10.1126/science.aaf5043

Warren, P. H. (2011). Stable-isotopic anomalies and the accretionary assemblage of the Earth and Mars: A subordinate role for carbonaceous chondrites. *Earth and Planetary Science Letters*, *311*, 93–100. https://doi.org/10.1016/j.epsl.2011.08.047

Weisberg, M. K., McCoy, T. J., & Krot, A. N. (2006). Systematics and evaluation of meteorite classification. In Lauretta, D. S., & McSween, H. Y. (Eds.), *Meteorites and the Early Solar System II* (pp. 19–52). Tucson: University of Arizona.

Weiss, B. P., Bai, X.-N., & Fu, R. R. (2021). History of the solar nebula from meteorite paleomagnetism. *Science Advances*, *7*, eaba5967. https://doi.org/10.1126/sciadv.aba5967

Weiss, B. P., Gattacceca, J., Stanley, S., Rochette, P., & Christensen, U. R. (2010). Paleomagnetic records of meteorites and early planetesimal differentiation. *Space Science Reviews*, *152*, 341–390. https://doi.org/10.1007/s11214-009-9580-z

Williams, J. P., & Cieza, L. A. (2011). Protoplanetary disks and their evolution. *Annual Review of Astronomy and Astrophysics*, *49*, 67–117. https://doi.org/10.1146/annurev-astro-081710-102548

Wölfer, E., Budde, G., & Kleine, T. (2020). Tungsten and molybdenum isotopic constraints on the age and origin of CH and CB chondrites. *Lunar and Planetary Science Conference*. LI, abstract #2445.

AGU Advances

Supporting Information for

What Can Meteorites Tell Us About the Formation of Jupiter?

Benjamin P. Weiss[1], William F. Bottke[2]

[1]Department of Earth, Atmospheric and Planetary Sciences, Massachusetts Institute of Technology, Cambridge, MA 02144, USA.

[2]Department of Space Studies, Southwest Research Institute, 1050 Walnut St, Suite 300, Boulder, CO 80302, USA

Contents of this file

Introduction

This supporting information provides a table to support the main article's methods and results.

Table S1. Temporal constraints on the growth of Jupiter

M ($M_\oplus$)	Growth Stage	Constraint	Technique	Ref.	t (Ma)	dM/dt ($M_\oplus$ Ma^{-1})
10-25	End of phase I	Accretion of carbonaceous bodies	Hf-W[1]	(Kruijer et al., 2017)	<1.3	>7.7 from 0 to 10 $M_\oplus$ >19.2 from 0 to 25 $M_\oplus$
50	Date 50$M_\oplus$ reached	Formation of CR chondrules	Al-Mg[2]	(Schrader et al., 2017)	>3.46	<18.5 from 10 to 50 $M_\oplus$ <11.6 from 25 to 50 $M_\oplus$
50		Formation of CR chondrules	Youngest U-Pb age with nominal CAI age[3]	(Amelin et al., 2010; Bollard et al., 2017; Connelly et al., 2012)	>3.42	<18.8 from 10 to 50 $M_\oplus$ <11.8 from 25 to 50 $M_\oplus$
50		Formation of CR chondrules	Youngest U-Pb with alternative CAI age[4]	(Bollard et al., 2017; Bouvier et al., 2011)	>3.80	<16.0 from 10 to 50 $M_\oplus$ <10.0 from 25 to 50 $M_\oplus$
50		Formation of CR chondrules	Hf-W[5]	(Budde et al., 2018)	>3.34	<19.6 from 10 to 50 $M_\oplus$ <12.3 from 25 to 50 $M_\oplus$
318	End of phase III	Magnetism of angrites	U-Pb with nominal CAI age[6]	(Amelin et al., 2010; Connelly et al., 2012; Tissot et al., 2017)	<3.94	>518 from 50 to 318 $M_\oplus$
318		Magnetism of angrites	U-Pb with alternative CAI age[7]	(Bouvier et al., 2011; Tissot et al., 2017)	<4.61	>225 from 50 to 318 $M_\oplus$
318		Magnetism of angrites	Al-Mg[8]	(Spivak-Birndorf et al., 2009) (Schiller et al., 2015)	<4.88 <5.03	>184 from 50 to 318 $M_\oplus$ >167 from 50 to 318 $M_\oplus$
318		Magnetism of CV chondrites	Mn-Cr[9]	(Doyle et al., 2015; Glavin et al., 2004)	<4.89	>183 from 50 to 318 $M_\oplus$
318		Formation of CB chondrules	U-Pb with nominal CAI age[10]	(Amelin et al., 2010; Bollard et al., 2015; Connelly et al., 2012; Johnson et al., 2016)	<5.08	>162 from 50 to 318 $M_\oplus$
318		Formation of CB chondrules	U-Pb with alternative CAI age[11]	(Bollard et al., 2015; Bouvier et al., 2011; Johnson et al., 2016)	<6.44	>88.9 from 50 to 318 $M_\oplus$

Notes: The first column lists the modeled mass of proto-Jupiter in units of Earth masses, the second column lists the corresponding approximate core accretion growth phase or event (phase I = formation of rocky core with final mass equal to the pebble isolation mass, 50$M_\oplus$ = time when proto-Jupiter reached 50$M_\oplus$, phase III = runaway gas accretion with final mass equal to Jupiter's present-day mass), the third column lists the physical process or meteorite record used to date this phase boundary or event, the fourth column lists the radiometric technique used, the fifth column lists the references for the radiometric constraint, the sixth column lists the age relative to the formation of CAIs in millions of years (Ma) (positive values = younger), and the seventh column lists the inferred mean growth rate of proto-Jupiter over the phase ending at this boundary assuming a linear growth rate during the phase. Our preferred age constraints are shaded in gray. The end of phase II, at which slow gas accretion reached the crossover mass, is predicted to be 25-50$M_\oplus$.

[1]Using upper limit on accretion age for carbonaceous bodies inferred from global differentiation ages constrained by ^{182}W data. Kruijer et al. (2017) proposed that this provides an upper limit on the time at which the carbonaceous and noncarbonaceous reservoirs first became isolated.
[2]Using (a) weighted mean Al-Mg age of 21 chondrules drawn from 9 chondrites minus (b) the 95% confidence interval referenced to the canonical CAI initial ^{26}Al/^{27}Al ratio of 5.23×10^{-5} (Jacobsen et al., 2008).
[3]Using youngest U-Pb age measured for CR chondrules [which Kruijer et al. (2017) proposed sets a lower limit on the time of mixing of the carbonaceous and noncarbonaceous reservoirs] referenced to the nominal weighted mean U-Pb CAI formation age of 4567.30 ± 0.16 Ma of Amelin et al. (2010) and Connelly et al. (2012). This is our preferred CR chondrule age because it is an absolute age and is referenced to a CAI age in the refereed literature.
[4]Same as footnote 3 but referenced to the alternative U-Pb CAI age of 4567.94 ± 0.21 Ma of Bouvier et al. (2011).
[5]Using weighted mean Hf-W age of (a) 38 subsamples from 4 CR chondrites minus (b) the 95% confidence interval.
[6]Calculated as the sum of: (a) weighted mean U-Pb age of the angrites D'Orbigny and Sahara 99555 referenced to the nominal U-Pb CAI-formation age (see footnote 3); (b) 95% confidence interval on the weighted mean U-Pb age

of these angrites and of the nominal U-Pb CAI age combined in quadrature. This is our preferred constraint on the end of phase III because it is an absolute age and is referenced to a CAI age in the refereed literature.

[7]Same as footnote 6 except using the alternative U-Pb CAI formation age (see footnote 4).

[8]Top and bottoms rows are calculated using the sum of the following: the volcanic angrites' mean initial $^{26}Al/^{27}Al$ ratio as measured by Spivak-Birndorf et al. (2009) and Schiller et al. (2015), respectively, and assuming the canonical CAI initial $^{26}Al/^{27}Al$ ratio (see footnote 2); (b) the 95% confidence interval on these Al-Mg ages.

[9]Calculated as the sum of: (a) weighted mean Mn-Cr age of fayalite in CV chondrite A-881317 relative to the D'Orbigny standard (b) the U-Pb age of D'Orbigny (Tissot et al., 2017); (c) the U-Pb age difference between D'Orbigny and the nominal U-Pb CAI-formation age (see footnote 3); (d) 95% confidence intervals of the Mn-Cr age and these two U-Pb ages combined in quadrature. Note this age is indistinguishable but has lower uncertainty than the I-Xe age of magnetite in the CV chondrite Kaba (Pravdivtseva et al., 2013).

[10]Calculated as the sum of: (a) weighted mean U-Pb age of chondrules from the CB chondrite Gujba referenced to the nominal weighted nominal U-Pb CAI-formation age (see footnote 3); (b) 95% confidence intervals of the weighted mean U-Pb age of these chondrules and of the nominal U-Pb CAI-formation age combined in quadrature.

[11]Calculated in the same way as the other estimate for CB chondrules (footnote 10) except using the alternative U-Pb CAI formation age (see footnote 4).